This article has been accepted for publication in a future issue of this journal, but has not been fully edited. Content may change prior to final publication. Citation information: DOI 10.1109/TIA.2017.2740850, IEEE Transactions on Industry Applications

Voltage and Reactive Power Control to Maximize the Energy Savings in Power Distribution System with Wind Energy

Rahul Anilkumar
Member, IEEE
Quanta Technology
428 13th Street
San Francisco, CA 94612, USA
kumar.rahulanil@gmail.com

Griet Devriese
Member, IEEE
Power Engineers
Clarkston, WA, USA
odditygriet@gmail.com

Anurag K Srivastava
Senior Member, IEEE
Washington State University
355 Spokane St.
Pullman, WA 99163, USA
asrivast@eecs.wsu.edu

***Abstract* – Commonly, voltage regulators and capacitor banks are used as control devices for voltage and reactive power (volt/VAr) control in distribution system. A specific mechanism can be developed using volt/VAr control for energy savings known as Conservation Voltage reduction (CVR). Active distribution system with high penetration of distribution generations (DG's) offers additional mechanism for volt/VAr control. The unique contribution of this paper is development of a computational algorithm for intelligent volt/VAr optimization and control of complex distribution networks with active participation from DG's, to maximize overall network energy savings through CVR. Proposed volt/ VAr optimization problem is solved to find the optimal voltage regulator settings, switched capacitor states and voltage magnitude of DG controlled bus. This work presents a unique coordinated volt/VAr architecture that can find application in Distribution Management System (DMS). Particle Swarm Optimization has been used, given compatibility with combinatorial variables, robustness in solving nonlinear optimization problems and ease of implementation. The results have been validated against an exhaustive search strategy for the IEEE 13 bus and IEEE 37 bus distribution system and also using commercial distribution software SynerGEE. Results are also presented for a utility feeder with detailed analysis.**

***Index Terms*-- Distributed Generation, DFIG, Energy Savings, Integrated Volt/Var Control (IVVC), Particle Swarm Optimization.**

I. INTRODUCTION

Recent studies revealed that there are 12 million distributed generation (DG) units installed across the United States, which is about one-sixth of the capacity of the nation's existing centralized power plants [1-3]. The realized benefits from these DGs connected at the distribution level include, improved network reliability, minimized energy losses, and an increase in the power supply capability within the existing infrastructure [4-5]. However, when a DG unit is interconnected to the distribution system, it can significantly change the system voltage profile and interact with step type voltage regulator and/or capacitor control operations [6-10].

Distributed wind generation units like Doubly Fed Induction Generator (DFIG) take advantage of power electronic converters and their different mode of control, to support the grid with additional reactive power at the point of common coupling. The IEEE 1547 standards form the basis for DG interconnection into the distribution network. In accordance with these standards, DGs should maintain a constant power factor close to unity at PCC. Additional switched capacitor bank support is allowed in order to meet this requirement [11]. Although these standards prohibit active voltage regulation, it is permissible to perform voltage regulation if a mutual agreement between the utility and DG owner exists [6]. Depending on the size of the DG, they can be operated either in power factor control mode, voltage control mode or voltage regulation mode [6]. Currently, the smaller DG units are controlled in power factor control mode, while the larger units generally operate with voltage control [1]. In the power factor control mode, the power factor is maintained unity at Point of Common Coupling (PCC), by modeling as a PQ bus with negative current injections.

Voltage control mode maintains voltage of PCC bus at a constant value, generally 1 p.u, whereas voltage regulating mode allows for active voltage regulation at the PCC bus, thereby accommodating additional VAr support in the network. These operations are restricted by the size of the DG converter, which is capable of generating or consuming reactive power within current limits ($-I_{max}$, $+I_{min}$) imposed by its rating [1]. While modeling these modes of operation, two methods can be adopted. For first one, local control can be added with the DG unit to maintain the voltage of PCC at a required value, based on the difference between reference voltage and the PCC voltage, while allowing the reactive power output from the Grid Side converter to operate in power factor control mode [1]. For the voltage regulating approach, the distribution power flow solution algorithm can account for PV bus in formulation by addition of the controlled voltage equation into the Jacobian matrix and consequently introducing reactive power as an additional state variable [12-14].

The volt/VAr problem has been formulated as an optimization problem to minimize the losses in the distribution network in [15]. The solution technique used to solve this problem is the genetic algorithm and the inequality constraints include the generator reactive capability limits. A

This article has been accepted for publication in a future issue of this journal, but has not been fully edited. Content may change prior to final publication. Citation information: DOI 10.1109/TIA.2017.2740850, IEEE Transactions on Industry Applications

multi-objective scenario based volt/VAr control algorithm is proposed in [16] which account for the stochastic behavior of renewable technologies while optimizing the network with capacitor banks and load tap changing transformers solved using the modified teaching learning algorithm. Synchronous distributed generation is considered in a coordinated control strategy with capacitor states and load tap changers to minimize network losses in [17]. The authors in [18] discuss new opportunities in DMS applications of volt/VAr control and feeder reconfiguration. The work in [19] proposes an algorithm to alleviate voltage control problem when installing distributed generation. The work in [20] proposes an optimized distributed control approach based on sensitivity analysis and on decentralized active/reactive power regulation which tries to minimize network losses and reactive power exchanged between the DG and distribution network. The authors of [21] modeled the volt/VAr problem in a stochastic framework by proposing a method to regulate the voltage profile of the operation planning the distribution network.

While developing a volt/VAr control scheme for an active distribution system, the operating characteristics of DG units and the complex behavior of different DG control modes should be taken into account to better understand their impact on the network state variables. Further there is a need to coordinate and control all VAr sources by accounting for the impact of DG parameters as a control variable in the problem formulation, while identifying the optimal operating states of the other control devices which include the switched capacitor states and voltage regulator settings [22, 23]. Most of the existing works focus on power factor control mode of operation, while optimizing the distribution network.

Original contributions of this paper are development of an intelligent computational algorithm for coordinated volt/VAr control considering the impact of different control modes of DG operation, while maximizing the energy savings of an active distribution system. Energy saving is achieved by lowering the voltage along the feeder with flatter voltage profile but keeping the voltage within allowable limits. Load consumption by voltage dependent load reduces by lowering the voltage and this mechanism is known as conservation voltage reduction (CVR). The problem has been solved for capacitor placement for any given feeder, and the operational stage by coordinated voltage control for maximum energy savings. Note that, this paper is focused on technical aspects and economic aspects have not been considered. During the capacitor placement stage, capacitor locations are determined using traditional loss sensitivity analysis. During operational stage, the proposed algorithm can optimally coordinate all the VAr sources in the network and solve for their control states, while ensuring the network security constraints are satisfied. The power factor control mode and voltage control mode of the DGs are analyzed as a part of this optimization problem by holding the associated parameters constant. However, in the voltage regulation mode, the voltage of the generator bus at PCC is added as a control variable into the optimization problem. Hence, in addition to switched capacitor states and VR settings, the optimum DG operating voltage is determined that maximizes the network energy savings.

The developed optimization algorithm has been tested on the IEEE 13 bus and IEEE 37 bus distribution test feeders. Cases have been simulated, with DG integration into the network, while identifying potential energy saving benefits of each DG mode of operation. The obtained results with and without DG are then validated using a commercial distribution planning tool, SynerGEE [24].

II. Problem Formulation

In this work, the overall energy savings of the active distribution system are maximized while determining the optimal operating states of different control devices. Energy savings can be realized in the form of kW energy savings, or kVA energy savings. The objective function is defined as follows:

$$Maximize\ ES = 100\%.\frac{P_{system_{base\ case}} - P_{system_i}}{P_{system_{base\ case}}} \quad (1)$$

Where ES denotes the energy savings, $P_{system_{base\ case}}$ represents the kW results obtained after solving the base case power flow without volt/VAr control, and P_{system_i} denotes the kW power flow results obtained for each 'i^{th}' possible operation with volt/ VAr control.

The objective is subject to the following inequality constraints

$$V_i^{min} \le V_i \le V_i^{max} \quad (2)$$

$$V_j^{min} \le V_j \le V_j^{max} \quad (3)$$

$$Q_j^{min} \le Q_j \le Q_j^{max} \quad (4)$$

$$0.95\ lagging\ \ \le PF_i \quad (5)$$

$$0.98\ leading\ \ \le PF_i \quad (6)$$

Where

V_i = Bus voltage for i^{th} load bus.

V_j = Bus voltage for j^{th} DG bus.

Q_j = Reactive power for j^{th} DG bus.

PF_i= Power factor for i^{th} load bus.

P_i^{calc} = Calculated real power for i^{th} load bus, "s" phase

S_i^s= Apparent power for i^{th} load bus, "s" phase

$$PF = {(P_i^{calc})^s}\Big/{S_i^s} \quad (7)$$

The equality constraints are the power flow equations.

$$(P_i^{calc})^s = V_{ri}^S(I_{rk}^{calc})^s + V_{mi}^S(I_{mi}^{calc})^s \quad (8)$$

$$(Q_i^{calc})^s = V_{mi}^S(I_{mk}^{calc})^s + V_{ri}^S(I_{ri}^{calc})^s \quad (9)$$

"V" and "I" denote the voltage and currents calculated at each bus. P^{calc} and Q^{calc} denote the calculated active and

This article has been accepted for publication in a future issue of this journal, but has not been fully edited. Content may change prior to final publication. Citation information: DOI 10.1109/TIA.2017.2740850, IEEE Transactions on Industry Applications

reactive power at each bus. Equations (2) and (3) represent voltage limits on the load and DG buses in the network. Eq. (3) is a part of the voltage regulation mode of DG operation. Eq. (4) denotes limits on the reactive power capability of the distributed generation buses in the network and is applicable to voltage control and voltage regulation mode of DG operation. Eqs. (5) and (6) are constraints applied to the power factor limits on the network load buses.

The control variables in this optimization problem are based on the control devices in the network, which include the states of the switching capacitors and the voltage regulator settings. In the voltage-regulating mode of DG control, the DG bus terminal voltage is added as an additional control variable into the optimization problem. It should be observed that this optimization problem is treated as a mixed integer non-linear optimization problem with discrete and continuous variables.

III. Solution Approach

Using traditional approaches like the branch and bound method, and exhaustive search strategy (which guarantee an optimal solution) would be the ideal choice to solve such an optimization problem. However, the prohibitive complexity associated with branch and bound method, and computational intensity associated with exhaustive search strategy cannot qualify them as candidate solutions because of their impracticality in real time volt/VAr control environments [2]. Hence the use of computational intelligence algorithms as search methods can be a key approach for such a problem. These methods are computationally less intensive, and achieve the optimal solution faster.

The proposed optimization problem is solved using Particle Swarm Optimization (PSO). The PSO algorithm must be capable of handling binary and continuous variables in order to identify the operating state of the network control variables. The development of PSO was inspired by the social behavior of a flock of birds and originally created to graphically simulate the unpredictable movement of a flock of birds. Listed below are the main advantages of PSO that are beneficial to a problem of this nature [25].

1. The search for optimal solution is faster for large-scale systems due to inherent nature of PSO making it an ideal candidate for real time applications. PSO also demonstrates capability of handling numerous constraints in optimization easily.
2. Dimension of search space is equal to number of control variables in optimization problem. The execution time is directly proportional to the dimension of search space.
3. PSO can be easily modified to handle combinatorial problems with both discrete and continuous variables.
4. PSO can handle mixed integer non-linear optimization problems.

The proposed algorithm is validated against an exhaustive search strategy in this work. The exhaustive search strategy is used to ensure the PSO parameters are optimally tuned, and the obtained results do not suffer from partial optimism, and provide only the global optimal solution. In PSO, each particle adjusts its trajectory based on its own experiences and those of the rest of the flock [26]. A possible solution to the problem in a *d* dimensional search space is characterized as a particle. The particle position vector is denoted by $x_i = (x_{i1}, x_{i2}, x_{i3}, \dots x_{id})$ and velocity vector is denoted as $v_i = (v_{i1}, v_{i2}, v_{i3}, \dots v_{id})$. The best position of the particle is stored as $p_i = (p_{i1}, p_{i2}, p_{i3}, \dots p_{id})$. Of these particles, the one with the best fitness value is denoted as the best global fitness value represented as *g*. The position and velocity vectors of each particle are updated in every iteration and in accordance with the current best particle's parameters. Equations (10) and (11) below represent the position and velocity vector update for each iteration.

$$v_{id} = w.v_{id} + c_1.rand.(p_{id} - x_{id}) + c_2.rand.(p_{gd} - x_{id}) \quad (10)$$

$$x_{id} = v_{id} + x_{id} \quad (11)$$

$$w^t = w^{t-1}.\beta \quad (12)$$

Where,

rand is a quasi-random number selected from a uniform space.

p_{id} is the best previous position of particle *i* on dimension *d*.

p_{gd} is the position of the best particle on dimension *d*.

d is the problem dimension size.

$c_1 = 2$ and $c_2 = 2$ are acceleration coefficients.

w is the inertia weight which is initialized as 0.9.

Equation (12) is the inertia weight update, which is updated when the position and velocity vectors are updated. $\beta = 0.975$ is the decrement factor [25].

The PSO steps are repeated until the maximum number of iterations or a predefined tolerance has been reached. In order to adapt the PSO to output binary results for the discrete control variables, the algorithm has been modified slightly. The position vector results are analyzed based on their percentage distribution in the interval [0, 1] and converted to binary.

The distribution power flow is used to evaluate the fitness value of each particle, and also meet the network constraints. The search space is initially populated with random solution obtained from one of the power flow solutions, based on the control variables. Initial population has to meet the constraints. Fig. 1 shows a flow chart of the PSO operation.

This article has been accepted for publication in a future issue of this journal, but has not been fully edited. Content may change prior to final publication. Citation information: DOI 10.1109/TIA.2017.2740850, IEEE Transactions on Industry Applications

IV. System Modeling

A. Distributed Generation

The model for distributed generation used in this work is a DFIG model [1]. The main components of a DFIG system include a wind turbine model, two VSCs connected back to back through a DC link comprising of the grid side converter (GSC) and the rotor side converter (RSC), and a Wound Rotor Induction Machine (WRIM). The RSC is coupled to the WRIM, while the GSC is coupled to the stator terminals using a transformer. Much work has been done in the area of DG modeling and its control [26-28]. While studying the volt/VAr problem, we need to accurately access the power outputs from the DG source at any point of time for a given wind speed.

The authors in [27] developed a simplified model for the VSCs and WRIM used in DFIG and based on their assumptions, similar equations have been used to model the remaining components of the wind energy conversion system in this work as shown in fig.2 . The ratings of the VSCs and DC link are 30% of the total rating of the DFIG.

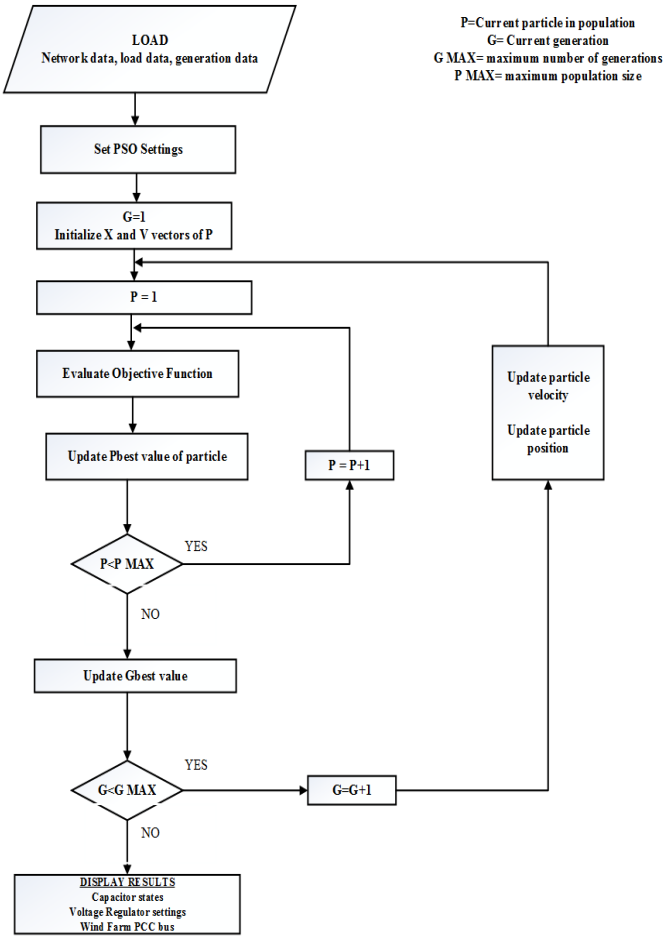

Fig. 1. Flow chart for Particle Swarm Optimization

In this model, the losses in the Grid side VSC, Rotor side VSC and transformer are denoted by the impedance Z_T. The DC link is assumed to be lossless. Due to this assumption,

$$P_{gsabc} = P_{rsabc} \tag{13}$$

Where P_{gsabc} and P_{rsabc} are the grid side and rotor side converter real power output, while "*abc*" represents the three phases. The real and reactive power output of the grid side VSC reaching the PCC is given by

$$P_{PCC\ abc} = real\left\{V_{Sabc}.\left(\frac{V_{Gabc}-V_{Sabc}}{z_T}\right)\right\} \tag{14}$$

$$Q_{PCC\ abc} = imag\left\{V_{Sabc}.\left(\frac{V_{Gabc}-V_{Sabc}}{z_T}\right)\right\} \tag{15}$$

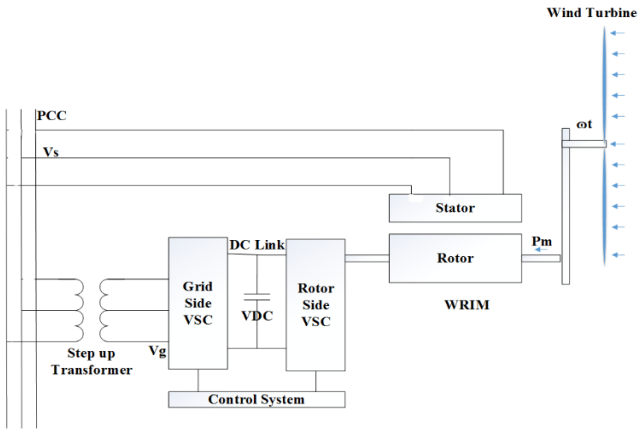

Fig. 2. DFIG model

Where $P_{PCC\ abc}$ represents the real power output of the GSC and $Q_{PCC\ abc}$ is the reactive power output of the GSC. V_{Sabc} denotes the supply side voltage, and V_{Gabc} the grid side voltage. While modeling the WRIM characteristics under unbalanced voltage conditions, symmetrical components have been used. Zero components have not been considered in this model because the WRIM is delta or ungrounded star connected. At stator frequency, the real and reactive power flow through the stator P_{st012} and Q_{st012} can be calculated by

$$P_{st012} = real\{V_{S012}.I^*_{S012}\} \tag{16}$$

$$Q_{st012} = imag\{V_{S012}.I^*_{S012}\} \tag{17}$$

Where, V_{S012} is the three phase supply voltages transformed into sequence components, and I_{s012} are the stator currents in their sequence components. At rotor frequency, the real power flow through the slip rings to voltage source converter is given by P_{rt012} and calculated as

$$P_{rt012} = real\{V_{r012}.I_{r012}\} \tag{18}$$

Where, V_{r012} is the rotor voltage transformed into sequence components, and I_{r012} are the rotor currents in their sequence components. The complete DFIG model under study combines equations (13)-(18), and the active power balance equation [28] that combines all the three elements of the DFIG with the stator and rotor copper winding losses

This article has been accepted for publication in a future issue of this journal, but has not been fully edited. Content may change prior to final publication. Citation information: DOI 10.1109/TIA.2017.2740850, IEEE Transactions on Industry Applications

P_{sl012} and P_{rl012} is given by

$$\sum P_{st012} + \sum P_{rt012} = \frac{P_m}{3} + (\sum P_{sl012} + \sum P_{rl012}) \quad (19)$$

By knowing the three-phase supply voltage V_{Sabc} and the wind speed v_{wind}, the power generated on each phase of the DFIG can be finally calculated as

$$P_{abc} = P_{Sabc} + P_{PCCabc} \quad (20)$$

$$Q_{abc} = Q_{Sabc} + Q_{PCCabc} \quad (21)$$

While modeling power factor control mode of the DFIG, the reactive power output $Q_{abc} = 0$ at the PCC bus, allowing the power factor to be maintained at unity. This can be modeled as a PQ bus in this work with negative P injections. While modeling voltage control modes in this formulation, PV bus modeling is included as a part of the Three Phase Current Injection Method (TCIM) power flow [29]. The DFIG PCC bus is considered as a PV bus to regulate or control voltage at PCC.

B. Distribution Power Flow

In this work, TCIM power flow is used to calculate real and imaginary parts of three-phase voltages of buses and it is valid for both balanced and unbalanced system conditions. The computational method used in this power flow is governed by [29]. PV buses have been modeled into the network using the equations from [30]. Equation (22) represents the augmented set of linearized equations used to accommodate PV buses into the power flow problem.

$$\begin{bmatrix} \Delta I_m^s \\ \Delta I_r^s \\ \hline \Delta V_k^s \end{bmatrix} = \begin{bmatrix} J & X \\ Z & 0 \end{bmatrix} . \begin{bmatrix} \Delta V_r^s \\ \Delta V_m^s \\ \hline \Delta Q_k^s \end{bmatrix} \quad (22)$$

Where, ΔI_r^s and ΔI_m^s represent the real and imaginary parts of the current mismatches for phases '*abc*'. The sub-matrix X is the partial derivative of these mismatches with the active power. ΔV_k^s and ΔQ_k^s represent the voltage and reactive power mismatches for phases '*abc*' of the PV bus. Sub-matrix Z is formed from the ratios of the real part of the 's' phase voltage phasor at bus '*k'* to the absolute value of 's' phase at bus '*k'*. ΔV_r^s and ΔV_m^s represent the real and imaginary parts of the voltage mismatches for phases '*abc*' at PQ buses in the network. Additional information pertaining to the TCIM power flow is available in [30].

$$\Delta Q_k^s = (Q_k^n)^s - (Q_k^{calc})^s \quad (23)$$

For voltage control mode, the DFIG model is initialized during the first iteration and Q_k^{calc} is obtained, which is then used to calculate the Q_k^n based on equation (22), relating ΔQ_k^s and the voltage mismatch ΔV_k^s. If the reactive power limits of the DG have been crossed during computation, violating the imposed constraints, it is fixed at the limiting value and the bus is now treated as a PQ bus. If after the power flow, the Q_g of this converted bus falls back within limits, the node is switched back into a PV node.

The TCIM power flow technique, first initialize the voltages at all the buses to 1 p.u. The DFIG model is subsequently introduced and used to compute active and reactive power. For convergence, the power mismatches are calculated and the tolerance is checked. If the solution has not converged, the Jacobian matrix is calculated in the very next step, following which the state variables are solved for and updated. This process continues till the tolerance is within range or the maximum number of iterations reach the limit.

C. Voltage regulator model

To model the voltage regulator, bus 1 has been converted to a PV bus closest to the substation.

TABLE I
Voltage Regulator Control Settings and Change in Voltage

Tap Setting	Voltage Change (%)	Voltage Change (p.u.)
16H	10.00%	1.10000 p.u.
15H	9.38%	1.09375 p.u.
14H	8.75%	1.08750 p.u.
13H	8.13%	1.08125 p.u.
12H	7.50%	1.07500 p.u.
11H	6.88%	1.06875 p.u.
10H	6.25%	1.06250 p.u.
9H	5.63%	1.05625 p.u.
8H	5.00%	1.05000 p.u.
7H	4.38%	1.04375 p.u.
6H	3.75%	1.03750 p.u.
5H	3.13%	1.03125 p.u.
4H	2.50%	1.02500 p.u.
3H	1.88%	1.01870 p.u.
2H	1.25%	1.01250 p.u.
1H	0.63%	1.00625 p.u.
1L	-0.63%	0.99375 p.u.
2L	-1.25%	0.98750 p.u.
3L	-1.88%	0.98125 p.u.
4L	-2.50%	0.97500 p.u.
5L	-3.13%	0.96875 p.u.
6L	-3.75%	0.96250 p.u.
7L	-4.38%	0.95625 p.u.
8L	-5.00%	0.95000 p.u.
9L	-5.63%	0.94375 p.u.
10L	-6.25%	0.93750 p.u.
11L	-6.88%	0.93125 p.u.
12L	-7.50%	0.92500 p.u.
13L	-8.13%	0.91875 p.u.
14L	-8.75%	0.91250 p.u.
15L	-9.38%	0.90625 p.u.
16L	-10.00%	0.90000 p.u.

This article has been accepted for publication in a future issue of this journal, but has not been fully edited. Content may change prior to final publication. Citation information: DOI 10.1109/TIA.2017.2740850, IEEE Transactions on Industry Applications

The basis of this model is the SEL 2431, consisting of 32 settings: 16 upper, a neutral and 16 lower taps [31]. Tapping on the series winding provides $\pm 10\%$ voltage adjustments. A position of 1H corresponds to a +0.625% increment from a base of 1 p.u. A position of 1L corresponds to a -0.625% decrement from the base of 1 p.u with a voltage of 0.99375. Similarly, a position of 16H leads to a 10% voltage change, with a new voltage of 1.1 p.u and a position of 16L down to 0.9 p.u.. Table I provides the VR model tap settings and associated voltage change.

D. Capacitor allocation and switching model

To determine capacitor locations during planning stage, loss sensitivity based approaches are applied inspired by [32] and [33]. Loss sensitivity factors are calculated for the base case and normalized voltage values are calculated. The base case considered is the network with DG operation in constant power factor control mode, which is also the most commonly found DG interconnection requirement. Selection of this base case helps in demonstrating the impact of additional VAr support from the DG and other modes of control, on pre-determined capacitor states of the network. In this work, only fixed capacitor sizes of 200 kVAr are considered. The loss sensitivity based factors determine the sequence in which buses are to be considered for compensation, and the normalized voltage values decide whether the buses need Q compensation or not [33].

In order to demonstrate proposed algorithm performance fixed step size capacitors are considered. The capacitors operate as a binary variable, switching between status ON (1) and OFF (0).

V. Simulation Results and Discussion

The developed algorithm is implemented on the IEEE 13 node distribution network and the IEEE 37 node distribution network. Results have been analyzed for the following cases.

1. Volt/VAr optimization with DG in power factor control mode [C1]
2. Volt/VAr optimization with DG in voltage control mode [C2]
3. Volt/VAr optimization with DG in voltage regulation mode [C3].

As discussed earlier, an exhaustive search strategy is also implemented which calculates the percentage energy savings for every option and chooses the option, which yields the highest energy savings. Although time consuming, computationally intensive and unsuitable for real time operation, there is great confidence in the result obtained through exhaustive search, thereby chosen as the ideal candidate for tuning of PSO parameters and results validation. For cases C1-C3, the results in table II shows the optimal control states obtained through particle swarm optimization technique and exhaustive search technique.

A. IEEE 13 bus distribution test system

Fig. 3 represents the IEEE 13 node test distribution feeder [34] modified to accommodate the optimization problem. The loading of the base test system has been increased by 20%. Also, 200 kVAr switched capacitors have been added to the network based on the placement approach discussed in earlier sections. These capacitor locations have been identified at buses 6, 12 and 13. The DFIG generator has been connected to bus 11 in this network through a 500 kVA transformer and rated for 0.5 MW. A wind speed, v_{wind} of 15m/sec is assumed, which can be changed to other values and varying with time. The voltage regulator is modeled at bus 1 which is the most upstream in the network. The energy saving results obtained along with corresponding control device operational states are discussed here for all three cases described earlier.

TABLE II
IEEE 13 BUS- C1- ENERGY SAVINGS RESULTS

	Exhaustive Search	PSO
Capacitor States	<1,1,1>	<1,1,1>
VR settings	<1H,1H,2H>	<1H,1H,2H>
Energy Savings kW ØA	3.264%	3.265%
Energy Savings kW ØB	4.143%	4.146%
Energy Savings kW ØC	3.142%	3.144%

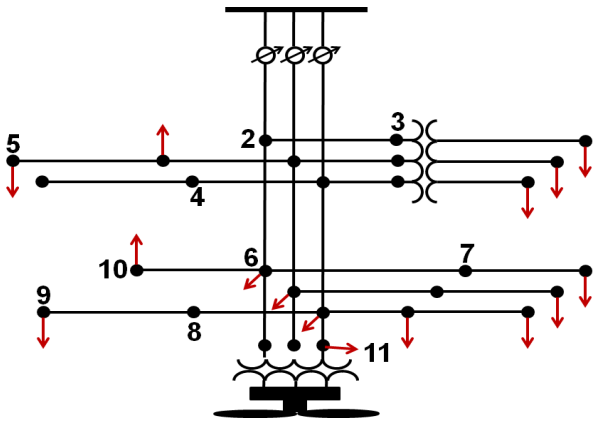

Fig. 3. IEEE 13 bus distribution network

TABLE III
IEEE 13 BUS- C2- ENERGY SAVINGS RESULTS

	Exhaustive Search	PSO
Capacitor States	<1,1,0>	<1,1,0>
VR settings	<N,1H,2H>	<N,1H,2H>
Energy Savings kW ØA	3.7832%	3.7832%
Energy Savings kW ØB	5.8978%	5.8978%
Energy Savings kW ØC	3.1345%	3.1345%

The impact of different DG controls on energy savings are clearly visible from the results of tables II, III and IV. Operating the DG in voltage control and voltage regulation mode prove to be the most beneficial to the network (C2 and

This article has been accepted for publication in a future issue of this journal, but has not been fully edited. Content may change prior to final publication. Citation information: DOI 10.1109/TIA.2017.2740850, IEEE Transactions on Industry Applications

C3 modes of operation). This is largely due to availability of more localized voltage control, and reduced switching among control devices in the network. Localized control helps with flatter voltage profile along the feeder and hence enhanced CVR. This is further enhanced by the locational benefit of DG resources closer to these devices. Due to the unbalanced loading conditions of the test system under consideration, different energy savings are obtained for individual phases. Another effect of unbalanced loading is the difference in voltages obtained for all phases of the DG bus. Care should be taken to ensure that large voltage imbalances don't occur as a result of DG integration into a differentially loaded network optimized under a regulating mode.

TABLE IV
IEEE 13 BUS- C3- ENERGY SAVINGS RESULTS.

	Exhaustive Search	PSO
Capacitor States	<1,0,0>	<1,0,0>
VR settings	<N,N,1H>	<N,N,1H>
Energy Savings kW ØA	7.913%	7.919%
Energy Savings kW ØB	8.353%	8.334%
Energy Savings kW ØC	7.103%	7.154%
DFIG bus Voltage ØA	1.009	1.008
DFIG bus Voltage ØB	1.012	1.014
DFIG bus Voltage ØC	1.009	1.009

Due to additional support from the DG source, reduced switching is observable in capacitor states. The results obtained are highly dependent on the nature of the system under consideration as well. Since the exhaustive search strategy explores every possible solution before determining the best operating state of the system, we can gather great confidence that the PSO has provided us the global optimal solution. PSO takes 34.67 seconds while exhaustive search takes 83.46 seconds to give optimal switching to maximize the savings.

B. IEEE 37 bus distribution test system

Three 1.5 MW wind generators operating at wind speed of 15 m/sec are installed at bus 775, 729 and 725 through a step up transformer rated for 1.5 MVA, and its low voltage side rating was changed from 0.48 kV to 2.4 kV. Switched Capacitors rated for 200 kVAr are placed at buses 733, 735, 701, 722 and 741 based on earlier discussed placement technique. Fig. 4 shows the IEEE 37 bus test [34].

TABLE V
IEEE 37 BUS- C1- ENERGY SAVINGS RESULTS

	Exhaustive Search	PSO
Capacitor States	<0,1,1,1,1>	<0,1,1,1,1>
VR settings	<3H,2H,1H>	<3H,2H,1H>
Energy Savings kW ØA	5.506%	5.503%
Energy Savings kW ØB	7.664%	7.667%
Energy Savings kW ØC	7.930%	7.930%

TABLE VI
IEEE 37 BUS-C2- ENERGY SAVINGS RESULTS

	Exhaustive Search	PSO
Capacitor States	<0,1,1,0,0>	<0,1,1,0,0>
VR settings	<1H,1H,N>	<1H,1H,N>
Energy Savings kW ØA	5.794%	5.792%
Energy Savings kW ØB	7.641%	7.662%
Energy Savings kW ØC	8.133%	8.135%

When tested on a larger system, the potential benefits of this approach are clearly distinct as shown in tables V, VI, VII. Taking into consideration the unbalanced nature of these systems, the differences in per phase savings can be attributed to the differential loading of the network. Larger savings are observed in the network with DGs integrated into them. This can be attributed to the additional VAr support from the DG units. Similar to the previous case studied, reduced capacitor switching is observed. The results in table VIII display results of optimized DFIG PCC bus voltages for case C3 comparing exhaustive search strategy (ESS) and PSO.

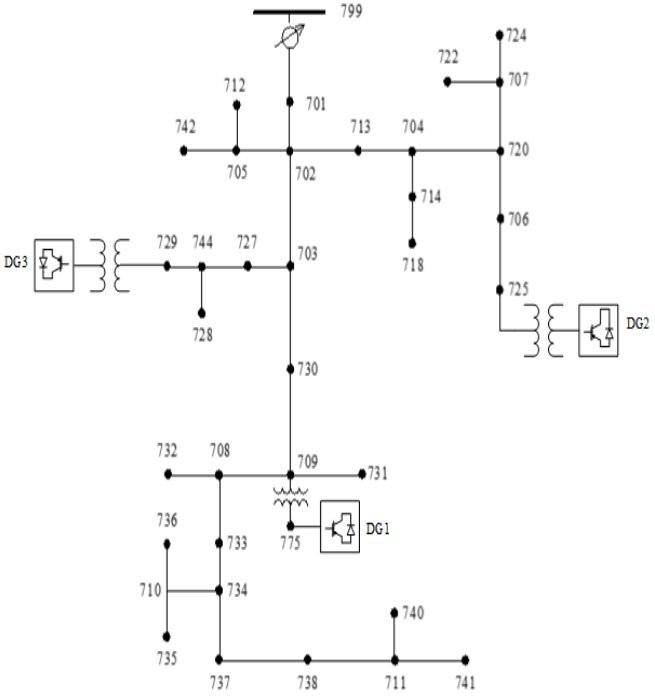

Fig. 4. IEEE 37 node distribution network

TABLE VII
IEEE 37 BUS- C3- ENERGY SAVINGS RESULTS

	Exhaustive Search	PSO
Capacitor States	<1,0,1,0,0>	<1,0,1,0,0>
VR settings	<1H,N,N>	<1H,N,N>
Energy Savings kW ØA	8.732%	8.736%
Energy Savings kW ØB	10.123%	10.123%
Energy Savings kW ØC	10.334%	10.319%

This article has been accepted for publication in a future issue of this journal, but has not been fully edited. Content may change prior to final publication. Citation information: DOI 10.1109/TIA.2017.2740850, IEEE Transactions on Industry Applications

TABLE VIII
DFIG BUS VOLTAGES FOR IEEE 37 BUS – C3

DFIG node	ØA		ØB		ØC	
	ESS	PSO	ESS	PSO	ESS	PSO
775	0.990	0.991	1.006	1.005	1.000	1.000
729	1.002	1.001	1.013	1.011	1.008	1.008
724	1.014	1.014	1.018	1.017	1.009	1.009

These reported results for energy savings are same for exhaustive search and PSO and only differs by less than 0.001-0.003 kW. Even if control devices setting are same, there is a very small difference exists in results given the numerical resolution of the solver developed in MATLAB. It is also important to note that voltage control is a localized problem, and inherently depends on the location of capacitor banks relevant to DG and voltage regulator. Therefore, it is not always necessary for less number of capacitors to be switched with DER. Similar observations can be made, depending on DG mode of volt/VAr control.

C. *Validation using SynerGEE Commercial Tool*

SynerGEE is commercial distribution planning tool commonly used by utilities to solve power flows [24]. SynerGEE has been used for a) interfacing PSO based optimization tool with industry grade software so utility can use the energy saving tool, b) to verify whether the energy savings assuming all control devices in service obtained from utility data versus those obtained as results from PSO algorithm result in larger energy savings. For validation analysis, the IEEE 13 bus distribution feeder has been modeled into the SynerGEE software tool. In order to validate the results obtained, the control states obtained for case C1 discussed in earlier section are used to evaluate system energy savings. The power factor control mode is modeled as a PQ bus using this tool, while running power flows without and with integrated volt/VAr control states. The cases run with volt/VAr control use the states of the control variables from the 13-bus network determined in section A of our simulation results. Using the results from both these cases, energy savings are calculated and compared to the results obtained from the developed algorithm.

TABLE IX
VALIDATION WITH SYNERGEE MODEL FOR IEEE 13 BUS

	PSO	SynerGEE
Capacitor States	<1,0,1>	<1,0,1>
VR settings	<1H,N,2H>	<1H,N,2H>
Energy Savings kW ØA	3.2653%	3.8437%
Energy Savings kW ØB	4.1429%	4.0145%
Energy Savings kW ØC	3.1444%	2.9987%

As observable from the results of Table IX, there is a minor difference in the results obtained from the proposed algorithm and SynerGEE. The difference is marginal with a mean difference of approximately 2%. The difference in results could be a result of different power flow techniques used in the proposed algorithm and SynerGEE software tool. Validation of proposed algorithm using commercial software tool, justifies its applicability in finding the optimal solution for volt/VAr applications to maximize energy savings.

D. *Implementation using AVISTA utilities real time feeder data.*

The developed PSO and Exhaustive search strategy (ESS) algorithm were also used to determine the optimal capacitor states and voltage regulator settings to maximize energy savings for utility feeders for a northwest energy provider located in Pullman, WA. Data for these utility feeders are not provided due to confidentiality reasons. It is important to note that no DER exists in the utility feeders and the control variables in the developed algorithm were accordingly modified. Real time feeder data provided by utility for several days of the year, available from PI-Server, were used to calculate potential energy savings with and without proposed volt/VAr control scheme.

The exhaustive search strategy and PSO techniques were implemented in SynerGEE Solver though VBA automated scripted. Tables X presents a comparison of results obtained from Exhaustive search and PSO algorithm for one specific day of the year. Figure 5 shows the results obtained with volt/VAr control optimization ON and with optimization algorithm OFF.

TABLE X
RESULTS FROM PULLMAN FEEDER 1

	PSO	SynerGEE
Capacitor States	<0,0,0>	<0,0,0>
VR settings	<11L,10L,11L>	11L,10L,11L>
Energy Savings kW [Average over all phases]	2.19%	2.1903%

Results obtained from real time feeder test clearly demonstrate the benefits in energy saving with and without volt/VAr control. From Pullman Feeder Case 1, close to 1500 kW in energy savings are obtained during peak hours of the day due to the developed strategy.

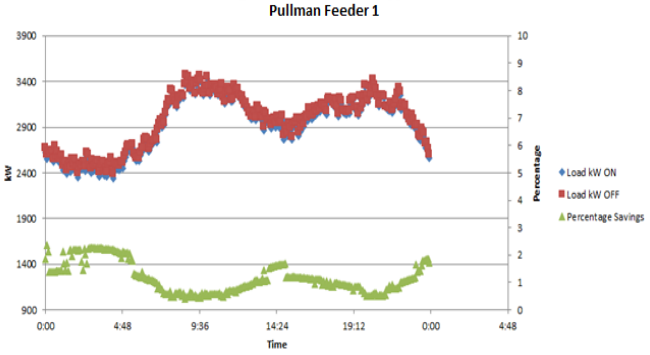

Fig. 5. Optimized energy savings using PSO for utility feeder 1

Similarly Table XI provides the results obtained for Feeder 2. Figure 6 shows the results obtained with optimal control ON

This article has been accepted for publication in a future issue of this journal, but has not been fully edited. Content may change prior to final publication. Citation information: DOI 10.1109/TIA.2017.2740850, IEEE Transactions on Industry Applications

for VVC with CVR and with optimal control OFF.

TABLE XI
RESULTS FROM PULLMAN FEEDER 2

	PSO	SynerGEE
Capacitor States	<0,1,0,0,0,0>	0,1,0,0,0,0>
VR settings	<12L,12L,11L>	<12L,12L,11L>
Energy Savings kW [Average over all phases]	2.10%	2.103%

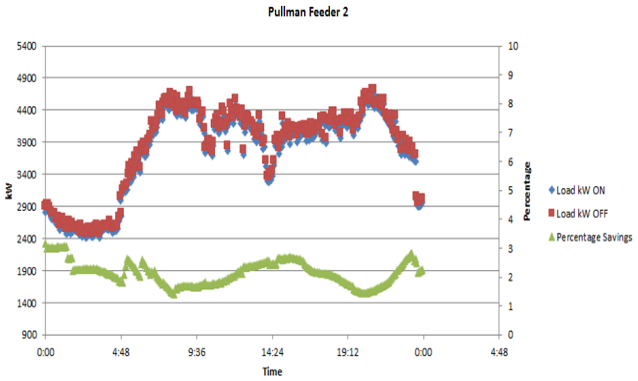

Fig. 6. Optimized energy savings for utility feeder 2

In both the utility feeder cases, energy savings is observed due to lower voltage controlled by all the considered control devices. Lower voltage results in lower energy consumption due to voltage dependent loads and irrespective of control model of distributed generation.

VI. Conclusions

In this work, an intelligent coordinated volt/VAr optimization approach is proposed to maximize energy savings for active distribution system with Distributed generation (DG). Impacts of different DG control schemes on distribution system volt/VAr controls have been analyzed. Developed algorithm can be used to identify the states of control devices in the distribution network, with the objective of maximizing the overall energy savings. The effect of DG for volt/VAr support is also taken into consideration while solving the optimization problem. Particle Swarm Optimization (PSO) was chosen as the solution approach and results have been validated for two modified IEEE test cases as well as for utility feeders. Based on PSO results validation, conclusions can be made on PSO reaching the global optimal solution and not sub-optimal solution. The complexity of the volt/VAr control problem in active distribution networks can be managed using the discussed solution technique.

The positive impact of DGs capable of regulating voltage at the grid is demonstrated. The impacts of DG controls have led to increased overall energy savings in the system. Based on the results obtained for cases with active DG participation, minimized capacitor switching operations are observed. In order to evaluate the performance of the developed algorithm, exhaustive search strategy and SynerGEE tool were used. The results from these techniques show satisfactory results.

The developed optimization problem can be expanded to include other objectives like minimizing the losses in the network, while focusing on maximizing supply from DGs to critical loads in the network other than maximizing the profits with demand response while meeting system constraints.

Acknowledgment

The authors acknowledge the support of AVISTA and the US Department of Energy to conduct this research work.

References

[1] Ackermann, T., “Wind Power in power systems” John Wiley and Sons Ltd., 2005.

[2] Al-Muhaini, M.; Heydt, G.T., "Evaluating Future Power Distribution System Reliability Including Distributed Generation," *IEEE Trans. on Power Delivery*, vol. 28, no. 4, pp. 2264-2272, Oct. 2013

[3] U.S Environmental Protection Agency, “Distributed Generation,” EPA, https://www.epa.gov/energy/distributed-generation#distributed Accessed in: June 2016.

[4] Tongdan, J; Yu, T; Cai Wen, Z; Coit, D.W., "Multicriteria Planning for Distributed Wind Generation Under Strategic Maintenance," *IEEE Transactions on Power Delivery*, vol. 28, no. 1, pp. 357-367, Jan. 2013.

[5] Abu-Mouti, F.S.; El-Hawary, M.E., "Optimal Distributed Generation Allocation and Sizing in Distribution Systems via Artificial Bee Colony Algorithm," *IEEE Transactions on Power Delivery*, vol. 26, no. 4, pp. 2090-2101, Oct. 2011.

[6] Walling, R.A.; Saint, R.; Dugan, R.C.; Burke, J.; Kojovic, Ljubomir A., "Summary of Distributed Resources Impact on Power Delivery Systems," *IEEE Transactions on Power Delivery*, vol. 23, no. 3, pp. 1636-1644, July 2008.

[7] Muttaqi, K.; Le, An; Negnevitsky, M; and Ledwich, G. "A Coordinated Voltage Control Approach for Coordination of OLTC, Voltage Regulator, and DG to Regulate Voltage in a Distribution Feeder," *IEEE Transactions on Industry Applications, vol.* 51, no. 2 pp. 1239-1248, 2015.

[8] Nian, H.; Shen, Y., Yang, H.; and Quan, Y. "Flexible Grid Connection Technique of Voltage-Source Inverter Under Unbalanced Grid Conditions Based on Direct Power Control," *IEEE Transactions on Industry Applications, v.* 51, no. 5 pp. 4041-4050, 2015.

[9] Win, T.; Hisada, Y.; Tanaka, T.; Hiraki, E.; Okamoto, M.; and Lee, S. "Novel Simple Reactive Power Control Strategy With DC Capacitor Voltage Control for Active Load Balancer in Three-Phase Four-Wire Distribution Systems," *IEEE Transactions on Industry Applications, vol.* 51, no. 5 pp. 4091-4099, 2015.

[10] Jain, B.; Jain, S.; and Nema, R. "Control strategies of grid interfaced wind energy conversion system: an overview," *Renewable and Sustainable Energy Reviews* vol. 47, pp. 983-996, 2015.

[11] IEEE 1547: Standard for Interconnecting Distributed Resources with Electric Power System, Standards Coordinating Committee, July 2003.

[12] Khushalani, S; Solanki, J. M.; Schulz, N. N.; “Development of Three Phase Unbalanced Power Flow Using PV and PQ Models for Distributed Generation and Study of the Impact of DG Models,” *IEEE Trans. on Power Systems*, vol. 22, no. 3, pp. 1019–1025, Aug. 2007.

[13] Blaabjerg, F; Teodorescu, R; Liserre, M; Timbus, A.V; “ Overview of Control and Grid Synchronization for Distributed Power Generation Systems”, *IEEE Transactions on Industrial Electronics*, vol. 53, no. 5, pp. 1898-1409, Oct. 2006.

[14] Ettehadi, M.; Ghasemi, H.; Vaez-Zadeh, S., "Voltage Stability-Based DG Placement in Distribution Networks," *IEEE Transactions on Power Delivery*, vol. 28, no. 1, pp. 171-178, Jan. 2013.

[15] Niknam, T; Ranjbar, A. M; Shirani, A. R; “Impact of Distributed Generation on Volt/VAR control in distribution networks”, *IEEE Bologna Power Tech Conference*, June 23-26, 2003.

[16] Niknam, T.; Zare, M.; Aghaei, J., "Scenario-Based Multiobjective Volt/Var Control in Distribution Networks Including Renewable

Energy Sources," *IEEE Transactions on Power Delivery*, vol. 27, no. 4, pp. 2004-2019, Oct. 2012.

[17] Viawan, F.A.; Karlsson, D., "Voltage and Reactive Power Control in Systems With Synchronous Machine-Based Distributed Generation," *IEEE Transactions on Power Delivery*, vol. 23, no. 2, pp. 1079-1087, April 2008.

[18] Roytelman, I.; Ganesan, V., "Coordinated local and centralized control in distribution management systems," *IEEE Transactions on Power Delivery*, vol. 15, no. 2, pp. 718-724, April 2000.

[19] Bollen, M. H J; Sannino, A., "Voltage control with inverter-based distributed generation," *IEEE Transactions on Power Delivery,* vol. 20, no. 1, pp. 519-520, Jan 2005.

[20] Calderaro, V.; Conio, G.; Galdi, V.; Massa, G.; Piccolo, A., "Optimal Decentralized Voltage Control for Distribution Systems With Inverter-Based Distributed Generators," *IEEE Transactions on Power Systems*, vol. 29, no. 1, pp. 230-241, Jan. 2014.

[21] Hong, Y.Y; Luo, Y.F "Optimal VAR Control Considering Wind Farms Using Probabilistic Load-Flow and Gray-Based Genetic Algorithms," *IEEE Transactions on Power Delivery*, vol. 24, no. 3, pp. 1441-1449, July 2009.

[22] Devriese, G; Shariatzadeh, F and Srivastava, A. K; "Volt/VAr Optimization with Energy Savings for Distribution System Using Intelligent Control", North American Power Symposium, Manhattan, KS, September, 2013.

[23] R. Anilkumar, G. Devriese, A. K Srivastava, "Intelligent volt/VAR control algorithm for active power distribution system to maximize the energy savings," in Proc. 2015 IEEE Ind. Appl. Soc. Ann. Meeting, Addison, TX USA, pp. 1 - 8, DOI: 10.1109/IAS.2015.7356832.

[24] SynerGEE Electric software tool, DNV-GL Group.

[25] Yuhuim, S; Eberhart, R; "A modified Particle Swarm Optimizer," Proceedings of *IEEE World congress on Computational Intelligence*, pp. 69-73, 4-9 May 1998.

[26] Lingling, F; Kavasseri, R.; Zhixin, L. M; Chanxia, Z, "Modeling of DFIG-Based Wind Farms for SSR Analysis," *IEEE Transactions on Power Delivery,* vol. 25, no. 4, pp. 2073-2082, Oct. 2010.

[27] Dadhania, A; Venkatesh, B; Nassif, A. B; Sood, V. K; "Modeling of doubly fed induction generators for distribution system power flow analysis", *Elsevier Journals on Electrical Power and Energy Systems*, 2013.

[28] Ostadi, A.; Yazdani, A.; Varma, R.K., "Modeling and Stability Analysis of a DFIG-Based Wind-Power Generator Interfaced With a Series-Compensated Line," *IEEE Transactions on Power Delivery,* vol. 24, no. 3, pp. 1504-1514, July 2009.

[29] Garcia, P. A. N; Pareira, J. L. R; Carneiro, S; da Costa, V. M; and Martins, N; "Three-Phase Power Flow calculations using the Current Injection Method", *IEEE Transactions on Power Systems*, vol. 15, no. 2, pp. 509-514, May 2000.

[30] Garcia, P. A. N; Pereira, J. L. R; Carneiro, S; Vinagre, M. P; "Improvements in the Representation of PV buses on Three-Phase Distribution Power Flow", *IEEE Transactions on Power Delivery*, vol. 19, no. 2, pp. 894–896, Apr. 2004.

[31] SEL, "SEL-2431 Voltage Regulator Control", Schweitzer Engineering Laboratories, May 2016.

[32] Paul, S.; Jewell, W., "Optimal capacitor placement and sizes for power loss reduction using combined power loss index-loss sensitivity factor and genetic algorithm," IEEE *Power and Energy Society General Meeting,* pp.1-8, 22-26 July 2012.

[33] Dehkordi, B. M.; Moallem, M.; Rezazadeh, S. J.; Amanifar, O.; Keivanfard, M., "Optimal capacitor placement and sizing in TABRIZ distribution system using loss sensitivity factors and particle swarm optimization (PSO)," *Proceedings of 17th Conference on Electrical Power Distribution Networks (EPDC),* pp.1-6, 2-3 May 2012.

[34] *IEEE Distribution test feeder working group, Test system available at: ewh.ieee.org/soc/pes/dsacom/testfeeders (Accessed in 2015).*